

## Resolution of the Orthopositronium-Lifetime Puzzle

R. S. Vallery,<sup>1,\*</sup> P. W. Zitzewitz,<sup>2</sup> and D. W. Gidley<sup>1</sup>

<sup>1</sup>*Randall Laboratory of Physics, University of Michigan, Ann Arbor, Michigan 48109-1120, USA*

<sup>2</sup>*Department of Natural Sciences, University of Michigan-Dearborn, Dearborn, Michigan 48128, USA*

(Received 18 March 2003; published 23 May 2003)

The long-standing discrepancy [G. S. Adkins, R. N. Fell, and J. Sapirstein, *Ann. Phys. (N.Y.)* **295**, 136 (2002)] between the theoretical calculations of the orthopositronium (*o*-Ps) annihilation decay rate ( $\lambda_T = 1/\text{lifetime}$ ) and some of the experimental measurements has been resolved. A focused beam of positrons incident on a special nanoporous silica film produces near-thermal energy *o*-Ps in vacuum that is slow enough to be virtually free of perturbing interactions. The fitted decay rate requires only a 500 ppm correction for nonthermal *o*-Ps effects. The new value of  $\lambda_T = 7.0404(10)(8) \mu\text{s}^{-1}$  is in excellent agreement with theory.

DOI: 10.1103/PhysRevLett.90.203402

PACS numbers: 36.10.Dr, 11.10.St, 12.20.Fv

Precision measurements of the annihilation decay rates of positronium (Ps) provide unique tests of quantum electrodynamics (QED) (see Ref. [1] and references therein). The triplet ground state decay rate,  $\lambda_T$ , of orthopositronium (*o*-Ps) has a colorful history [1] of inconsistent experimental results and poor agreement with theoretical calculations, the so-called *o*-Ps lifetime puzzle [2] (the lifetime,  $1/\lambda_T$ , is about 142 ns). The theoretical value has recently been solidified by completion of the full second order in  $\alpha$  QED corrections ( $\sim 230$  ppm) to yield [1,3]  $\lambda_T$  (theory) =  $7.039\,979(11) \mu\text{s}^{-1}$  (1.6 ppm) which includes additional higher-order logarithmic terms [2]. There is no longer any concern that the second order corrections might be large ( $\sim 1000$  ppm) and positive. (It is interesting to note that there is no corresponding *para*-positronium lifetime puzzle as the ground state singlet decay rate measured in a buffer gas [4] is in excellent agreement with theory [5] at the 215 ppm level of precision.) The fact that the QED theoretical value of  $\lambda_T$  has been lower than the most precisely measured values has spawned numerous (null) experiments [6] to search for exotic, non-QED *o*-Ps decay processes involving axions, C-odd bosons, millicharged particles, forbidden numbers of gamma rays, and a mirror universe [7]. In this Letter, we present the results of a new measurement of  $\lambda_T$  that definitively resolves the *o*-Ps lifetime puzzle.

The most precise measurements of  $\lambda_T$  using a buffer gas [8] and a vacuum technique [9] are  $7.0514(14) \mu\text{s}^{-1}$  (200 ppm) and  $7.0482(16) \mu\text{s}^{-1}$  (230 ppm), respectively. They are 1200–1600 ppm above theory and a more recent measurement [10] performed in silica powders,  $7.0399(26) \mu\text{s}^{-1}$  (370 ppm). The Michigan buffer gas experiment [8] has been shown to be subject to the problem of incomplete Ps thermalization [11] in low-pressure gases, and this value should be corrected downward by at least 700 ppm. The Tokyo experiment [10] in a fine-grained insulating powder could be subject to small Stark shifts that reduce the decay rate and are not accounted for in their technique, but the experiment primarily needs improved statistical precision. The 1990

Michigan vacuum experiment [9], wherein *o*-Ps is formed in an evacuated cavity using a low-energy beam of positrons, is attractive in eliminating gaseous and powder formation media. It suffered statistically and systematically from the presence of other intermediate lifetime *o*-Ps decay processes that required fitting the decay spectrum after 450 ns where only 4% of the *o*-Ps decays remain. After further research on this additional decay process [12], we have improved the vacuum technique and performed a new, more accurate measurement of  $\lambda_T$ .

The positron beam and timing electronics are similar to that described in Ref. [9]. Briefly, a 35 mCi <sup>22</sup>Na source is used to generate a primary positron beam of about  $4 \times 10^5$  e<sup>+</sup>/s that is electrostatically focused onto a 3 mm diameter Ni foil remoderator. A secondary beam of  $\sim 4 \times 10^4$  e<sup>+</sup>/s is generated from reemitted positrons and about 15% of these are time tagged by detecting secondary electrons ejected from the remoderator by the incoming positrons. The secondary beam has been improved to permit delivery of the positron beam onto the Ps formation surface over a wide range of implantation energies (1–5 keV), a key to performing systematic tests. The Ps formation and confinement cavity has been completely redesigned as shown in Fig. 1. New, more efficient annihilation gamma detectors (fast plastic scintillator) are centered on a small, two-chambered cavity. Timed positrons are electronically gated through a final lens that focuses them through two apertures into the second chamber. Electric fields from the biased cavity walls deflect the beam onto a special (see below) porous film where Ps is formed with 30%–33% efficiency. Unlike the 1990 experiment, there is no MgO powder fumed on the aluminum cavity walls. The time between the gated injection of positrons and the subsequent detection of one of the *o*-Ps annihilation gamma rays is measured and accumulated as a decay histogram. As in previous measurements, the decay rate is the fitted exponential slope of this decay spectrum and represents the total rate of *o*-Ps disappearance into all possible modes of decay.

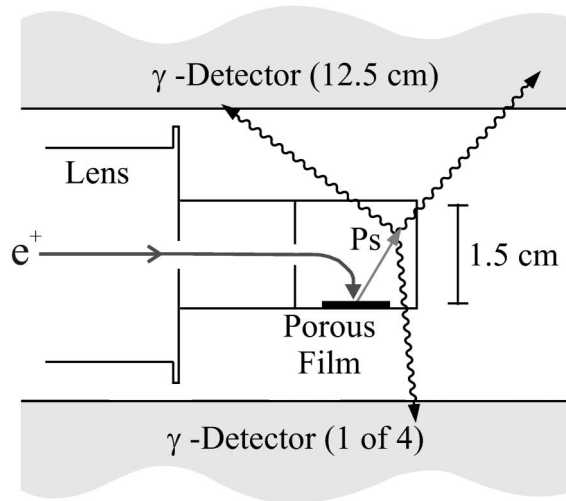


FIG. 1. The *o*-Ps formation and confinement region. The time-tagged positron beam is focused through apertures of 4 and 3 mm, respectively, and then deflected into a porous silica film where  $\sim 30\%$  form *o*-Ps. After many collisions in the interconnected 3.3 nm pores, most of the *o*-Ps that escapes the film is nearly thermalized and, hence, too slow to escape from the cavity or annihilate in wall collisions.

The most significant improvement over the 1990 experiment is the use of a porous silica film as the Ps formation target. Developed as low-dielectric constant materials by the microelectronics industry, these 1  $\mu\text{m}$ -thick films have pores that are several nm in diameter and fully interconnected to form a pore network [13]. A beam of keV positrons stop in the dense silica matrix and form Ps that is expelled into the pores with a couple eV of kinetic energy. With a mean-free path of 3.3 nm, Ps is able to diffuse through the pore network over distances much longer than the film thickness and escape through the surface into vacuum [13]. Having suffered on the order of  $10^4$ – $10^6$  collisions with the silica pore walls (depending on implantation depth), the Ps approaches thermal equilibrium. (Ps confined to the pores by a thin capping layer does indeed fully thermalize since the fitted lifetime is observed to have the expected strong dependence on the film's temperature [13].) We confirmed this in a separate time-of-flight experiment of Ps emitted into vacuum from a similar porous film. The energy distribution is nominally that of Maxwell-Boltzman emission (with an effective  $kT = 35$ – $40$  meV) joined with a high-energy tail (see Fig. 2). This tail of thermalizing Ps extends out at least to  $\sim 2$  eV, the energy at which Ps (formed from thermalized positrons in the silica) is expelled into the pores. In addition, there is a low-intensity higher-energy tail of 2–20 eV Ps formed from back-scattered positrons that never approached thermalization [12]. These Ps events are distinct from the thermal and epithermal Ps that has diffused out of the film pores and will be considered later.

There are several important consequences of having near-thermal Ps in the cavity. This Ps moves an average of

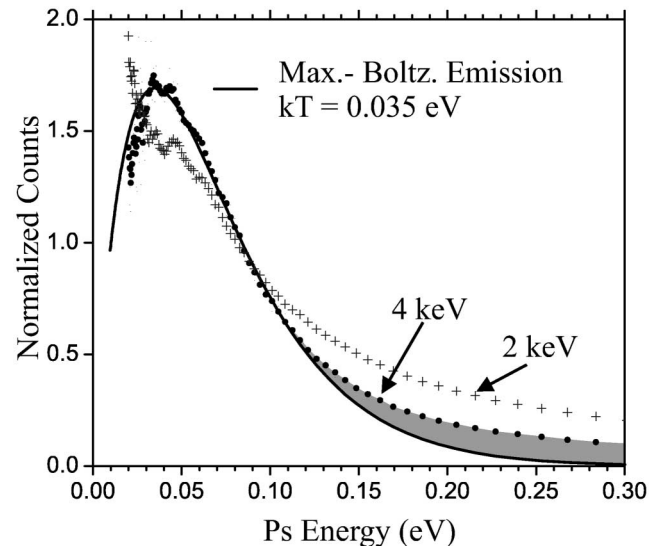


FIG. 2. The energy distribution of *o*-Ps emitted from a typical porous silica film. Note that higher energy positrons implanted more deeply (solid circles) in the film produce more thermalized *o*-Ps with fewer events in the epithermal tail.

only 1–2 cm in a lifetime and thus the surrounding cavity should have comparably small size in order to confine Ps to a region of highly uniform detection efficiency. (Ps cannot be allowed to move over several lifetimes into regions of systematically different gamma detection efficiency as this would modulate the lifetime spectrum and distort the fitted decay rate.) More importantly, even in a small cavity Ps makes only 1–3 wall collisions per lifetime and thus collisional wall quenching is negligible. (The Ps can clearly survive of order  $10^6$  collisions in diffusing through the silica film and a few more collisions with the alumina cavity surface is negligible.) Thus, thermal and epithermal Ps (energy  $< 2$  eV) sealed in a 1 cm cavity affords us the opportunity, in principle, to measure the vacuum decay rate directly without extrapolations. In practice, however, our cavity must have an aperture for the positron beam to enter. The escape/disappearance of some Ps through this aperture into regions of lower gamma detection efficiency (the major systematic effect in the 1990 experiment) systematically increases the fitted total disappearance rate of *o*-Ps and must be addressed.

With the above effects in mind, the double-chambered cavity, shown in Fig. 1, was designed. Each chamber is a cube with a side length of 1.5 cm corresponding to a mean-free path of 1.0 cm. The two-chamber design is based on the concept of differential pumping—i.e., the inner 3 mm diameter aperture is small enough to allow  $< 1\%$  of the thermal Ps to escape from the Ps formation chamber. The subsequent escape probability from the outer (second) chamber is 1%–2%, thus reducing the thermal Ps escape probability through both apertures to be less than 200 ppm. The tail of epithermal Ps will have higher escape probability, but Monte Carlo simulations

indicate that the overall disappearance effect of 0–2 eV Ps on the fitted value of  $\lambda$  is expected to be less than 200 ppm. Ps *transfer* over time between the two chambers has no effect because the gamma detectors are centered on the dividing bulkhead rendering the two chambers to be mirror images of each other. There are small (1%–2%) axial and radial gradients in detector efficiency over each chamber, but simulations indicate that the time-dependent “filling” of the formation chamber is complete in less than 200 ns (after which Ps is effectively averaging over the gamma detector gradients).

The two-chambered cavity is designed to have negligible Ps wall quenching and minimal entrance aperture effects for the Ps with kinetic energy less than 2 eV. However, this is not the case for the 2–20 eV tail of the Ps energy distribution. The origin(s) of this “backscattering” component is backscattered or very shallowly implanted positrons that capture an electron at the film surface to produce Ps with a broad range of energies. Production of this high-energy Ps that does not undergo thermalizing collisions within the film pores is well documented in the literature dealing with positron beams (see Ref. [12] and references therein).

The decay spectrum and relative intensity of the backscattered Ps events can be isolated by investigating *non-porous* films where there is no outdiffusion of low-energy Ps. We replaced the porous silica film with a thermal oxide-grown dense silica film. The resulting backscattered Ps typically produces two fitted lifetime components [12] in the cavity: a fast moving (and fast decaying, presumably by dissociation) component with a distribution of lifetimes in the 5–20 ns range and longer-lived, several eV Ps with lifetimes predominately in the 70–140 ns range. The fast Ps component decays away prior to fitting the decay rate for times after 150 ns and, hence, can be ignored, but the effect of the longer-lived components for fits beginning as far out as 500 ns can be clearly seen in Fig. 3. Fortunately, the relative intensity of these events can be controlled by the positron beam implantation energy [12],  $E$ , as roughly  $1/E$ . Thus, we have acquired decay rate spectra at positron beam energies of 1–5 keV using both the porous and the nonporous films. The nonporous film data were used in two complementary ways to remove the collisional quenching effect of the backscattered component.

In the first method, the decay rates fitted at  $t = 250$  ns in the full porous film spectrum are plotted versus the measured relative intensity of the backscattered Ps component (see Fig. 4). We assume the perturbation in the fitted decay rate should be linear in this relative intensity and extrapolate to zero backscattering. However, the backscattered Ps decay spectrum is not exponential in time (it is a broad distribution of exponentials). A second method is used to remove backscattered Ps directly from the time histogram prior to fitting the decay rate. From the full porous film spectrum (slow Ps plus backscattered Ps), an appropriately normalized dense oxide spectrum

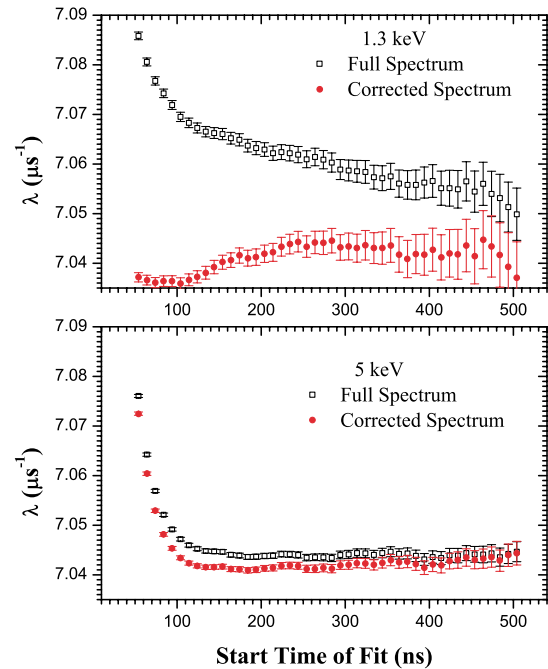


FIG. 3 (color online). The fitted decay rate as a function of the start time of the fit for two of the positron implantation energies used in this measurement. The decay rate for the full spectrum (of all *o*-Ps decays) has a higher decay rate at lower beam energy due to the increased relative intensity of the backscattering component. The corrected spectra have an appropriately normalized pure backscattering spectrum subtracted.

(backscattered Ps only) is subtracted to produce a corrected spectrum of purely slow Ps decay. The resulting fits of the corrected spectrum are included in Fig. 3. The corresponding fits at  $t = 250$  ns are also plotted in Fig. 4.

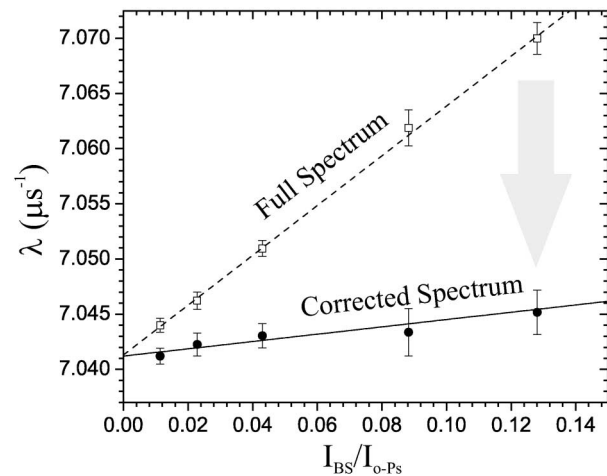


FIG. 4. The fitted decay rates at  $t = 250$  ns for a range of Ps implantation energies, plotted as a function of backscattered Ps over thermal *o*-Ps ( $I_{BS}/I_{o-Ps}$ ). A linear fit to the full spectrum decay rates is made to remove the effect of the backscattered *o*-Ps. The decay time spectra are also corrected directly for backscattering by subtracting an appropriately scaled backscattering spectrum from the full spectrum.

This second method assumes that the spectrum of backscattered Ps from the dense silica is identical to that from the porous silica, a reasonable but not precise approximation. Hence, extrapolation to zero backscattering for this corrected spectrum as shown in Fig. 4 is appropriate and yields  $7.0412(8) \mu\text{s}^{-1}$ . This intercept is systematically consistent at 30 ppm with that for the full spectrum extrapolation.

To determine the vacuum decay rate, we need to make a small additional correction for the effect of the disappearance of Ps that has bounced through both apertures. Simulations indicate this effect should be about 100–300 ppm and is quite sensitive to the relative intensity of epithermal Ps. To check this, we increased the first aperture diameter from 4 to 8 mm and acquired spectra at 5 and 2 keV beam energy. The aperture disappearance effect is deduced to be  $0.0008(6) \mu\text{s}^{-1}$  ( $115 \pm 85$  ppm). Our new value for the *o*-Ps decay rate is then  $\lambda_T = 7.0404(10)(8) \mu\text{s}^{-1}$ , where the first error is the statistical error of 140 ppm and the second error of 115 ppm represents a combined systematic error associated with the above extrapolation procedures and selection of the fitted value of the decay rate at 250 ns. Errors due to time calibration, spectrum linearity, and multiple *o*-Ps events [8] are negligible.

Our current value for  $\lambda_T$  using a porous silica thin film for production of near-thermal Ps is in excellent agreement with theory at a combined level of precision of 180 ppm. It also agrees well with the Tokyo [10] experiment. There is no longer an *o*-Ps lifetime puzzle. The problem with the 1990 vacuum experiment [9] is that it failed to correctly account for and extrapolate over the *intensity* of the backscattered Ps component. The Michigan group performed the extrapolations of the fitted decay rates vs the size of the confinement cavities (hence, the wall collision rate) and versus the entrance aperture area to account for Ps disappearance (see Ref. [9]), but kept the beam energy constant at a low value of 700 eV to keep the Ps formation high on the fumed MgO surface. Not realized at the time was the need to extrapolate in the positron beam implantation energy (and, hence, in the intensity of the perturbing, nonexponential backscattered Ps component) as done in the present measurement. The fits shown in the top panel of Fig. 3, obtained at low positron implantation energy, clearly illustrate the problem encountered in the 1990 experiment. Even though the decay rate appears to asymptotically approach a constant value for fits beyond  $t = 450$  ns as in Ref. [9], the backscattered Ps component still raises the fitted decay rate at *all* fitting times. Simulations confirm that increasing cavity size (decreasing the wall collision rate) allows this component to persist at longer and longer times. The extrapolation in the intensity of the nonexponential back-

scattered Ps component is essential to eliminate its effect on the fitted decay rate.

In summary, the major systematic effect in this experiment is the backscattered *o*-Ps at approximately 2–20 eV that requires a 350 ppm correction (at 5 keV beam energy) for collisional annihilation on the cavity walls. Epithermal *o*-Ps extending up to  $\sim 2$  eV requires a 100–200 ppm correction for escape from the confinement cavity. We are continuing data collection with the goal of reducing both the 115 ppm systematic error related to backscattered Ps and the 85 ppm uncertainty in the cavity aperture effect. Our final value of  $\lambda_T$  should achieve statistical and systematic uncertainties that are each  $\leq 100$  ppm.

We thank Mark Skalsey, G.W. Ford, Ralph Conti, William Frieze, Aaron Leanhardt, Jianing Sun, Jason Engbrecht, and Yifan Hu for many useful discussions. We thank the National Science Foundation Grant No. PHY-9731861 and the University of Michigan for supporting this research. We are grateful to International Sematech for continuing support of low-dielectric porous film research.

---

\*Electronic address: vallery@umich.edu

- [1] G. S. Adkins, R. N. Fell, and J. Sapirstein, *Ann. Phys. (N.Y.)* **295**, 136 (2002).
- [2] B. A. Kniehl and A. A. Penin, *Phys. Rev. Lett.* **85**, 1210 (2000); **85**, 3065 (2000); R. J. Hill and G. P. Lepage, *Phys. Rev. D* **62**, 111301 (2000); K. Melnikov and A. Yelkhovsky, *Phys. Rev. D* **62**, 116003 (2000).
- [3] G. S. Adkins, R. N. Fell, and J. Sapirstein, *Phys. Rev. Lett.* **84**, 5086 (2000).
- [4] A. H. Al-Ramadhan and D. W. Gidley, *Phys. Rev. Lett.* **72**, 1632 (1994).
- [5] G. S. Adkins, R. N. Fell, and J. Sapirstein, *Phys. Rev. A* **63**, 032511 (2001).
- [6] M. Skalsey, *Mater. Sci. Forum* **255-2**, 209 (1997).
- [7] R. Foot and S. Mitra, *Phys. Rev. D* **66**, 061301 (2002), and references therein.
- [8] C. I. Westbrook, D. W. Gidley, R. S. Conti, and A. Rich, *Phys. Rev. A* **40**, 5489 (1989).
- [9] J. S. Nico, D. W. Gidley, A. Rich, and P. W. Zitzewitz, *Phys. Rev. Lett.* **65**, 1344 (1990).
- [10] S. Asai, S. Orito, and N. Shinohara, *Phys. Lett. B* **357**, 475 (1995); O. Jinnouchi, S. Asai, and T. Kobayashi, hep-ex/0011011.
- [11] M. Skalsey, J. J. Engbrecht, R. K. Bithell, R. S. Vallery, and D. W. Gidley, *Phys. Rev. Lett.* **80**, 3727 (1998).
- [12] D. W. Gidley, D. N. McKinsey, and P. W. Zitzewitz, *J. Appl. Phys.* **78**, 1406 (1995).
- [13] D. W. Gidley, W. E. Frieze, T. L. Dull, A. F. Yee, E. T. Ryan, and H.-M. Ho, *Phys. Rev. B* **60**, R5157 (1999).